

**Electronic Supplementary Information (ESI)**

Shaping Particle Size Distribution of a Metastable Polymorph in  
Additive-assisted Reactive Crystallization by  
the Taguchi Method

Hung Lin Lee, Chia Ling Yang and Tu Lee\*

Department of Chemical and Materials Engineering, National Central University

300 Zhongda Road, Zhongli District, Taoyuan City 320317, Taiwan R.O.C.

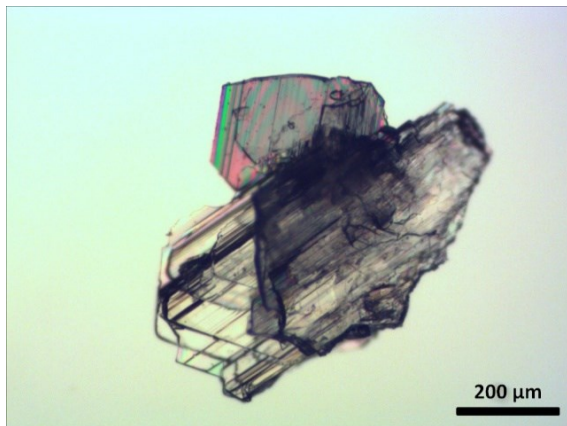
---

\* Corresponding Author. Tel: +886-3-4227151 ext. 34204. Fax: +886-3-4252296.

Email: [tulee@cc.ncu.edu.tw](mailto:tulee@cc.ncu.edu.tw)

**Table S1.** Form space of *L*-glutamic acid (*L*-GLU) at 25 °C.

	<i>n</i> -heptane	ethyl Acetate	toluene	methyl <i>tert</i> -butyl ether (MTBE)	methyl ethyl ketone (MEK)	chloroform	tetrahydrofuran (THF)	<i>N,N</i> -dimethylaniline (DMA)	acetone	1,4-dioxane	nitrobenzene	<i>n</i> -butyl alcohol	isopropyl alcohol	benzyl alcohol	acetonitrile	ethanol	dimethyl sulfoxide (DMSO)	methanol	water	
<ul style="list-style-type: none"> <li><span style="display: inline-block; width: 15px; height: 10px; background-color: #003366; border: 1px solid black;"></span> good-cosolvent</li> <li><span style="display: inline-block; width: 15px; height: 10px; background-color: #ffffff; border: 1px solid black;"></span> bad-cosolvent</li> <li><span style="display: inline-block; width: 15px; height: 10px; background-color: #008000; border: 1px solid black;"></span> antisolvent</li> <li><span style="display: inline-block; width: 15px; height: 10px; background-color: #ffff00; border: 1px solid black;"></span> pure good-solvent</li> <li><span style="display: inline-block; width: 15px; height: 10px; background-color: #ff0000; border: 1px solid black;"></span> pure bad-solvent</li> <li><span style="display: inline-block; width: 15px; height: 10px; background-color: #808080; border: 1px solid black;"></span> immiscible pairs</li> </ul>																				
<i>n</i> -heptane																				
ethyl acetate																				
toluene																				
methyl <i>tert</i> -butyl ether (MTBE)																				
methyl ethyl ketone (MEK)																				
chloroform																				
tetrahydrofuran (THF)																				
<i>N,N</i> -dimethylaniline (DMA)																				
acetone																				
1,4-dioxane																				
nitrobenzene																				
<i>n</i> -butyl alcohol																				
isopropyl alcohol																				
benzyl alcohol																				
acetonitrile																				
ethanol																				
dimethyl sulfoxide (DMSO)																				
methanol																				
water																				



(a)



(b)

**Figure S1.** OM images of  $\beta$ -GLU crystals obtained by (a) rapid and (b) slow cooling.

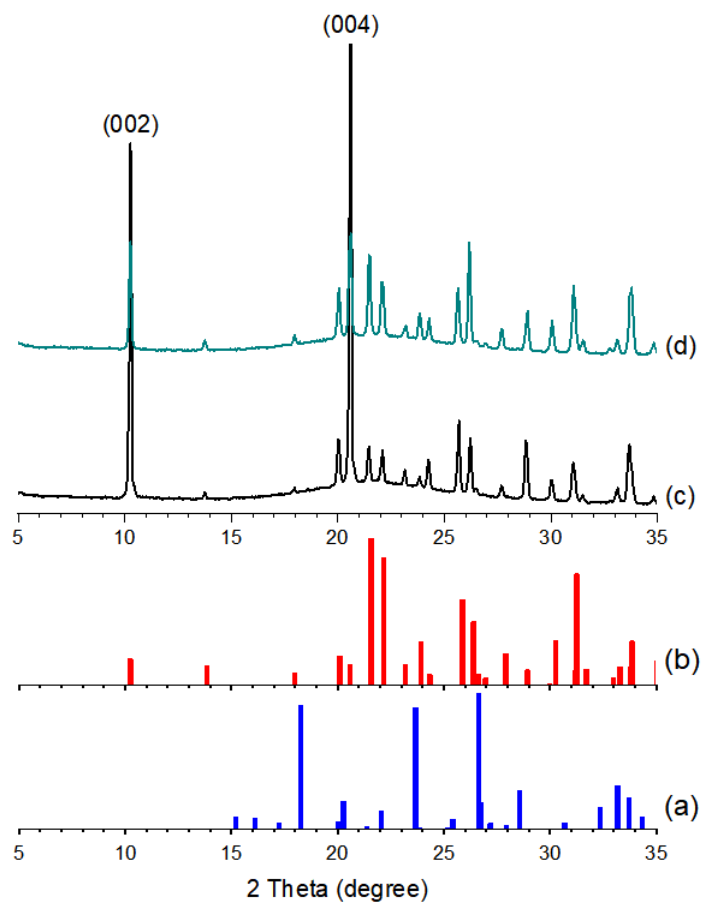


**Figure S2.** Theoretical patterns of (a)  $\alpha$ -GLU and (b)  $\beta$ -GLU acquired from the Cambridge Crystallographic Data Centre (CCDC) with CCDC codes: LGLUAC02 and LGLUAC01, respectively. PXRD patterns of (c-d)  $\beta$ -GLU crystals obtained by (c) rapid and (d) slow cooling.

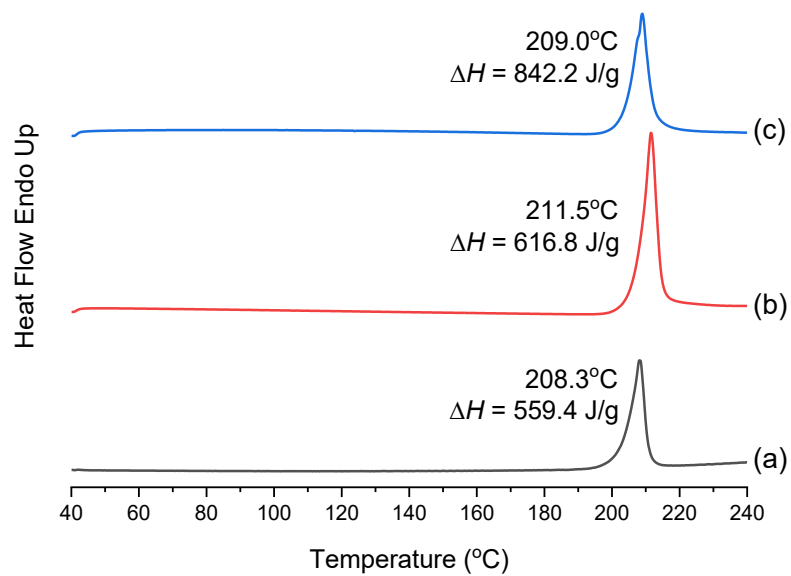


**Figure S3.** DSC scans of (a) purchased and (b-c) our prepared  $\beta$ -GLU crystals obtained by (b) rapid and (c) slow cooling.

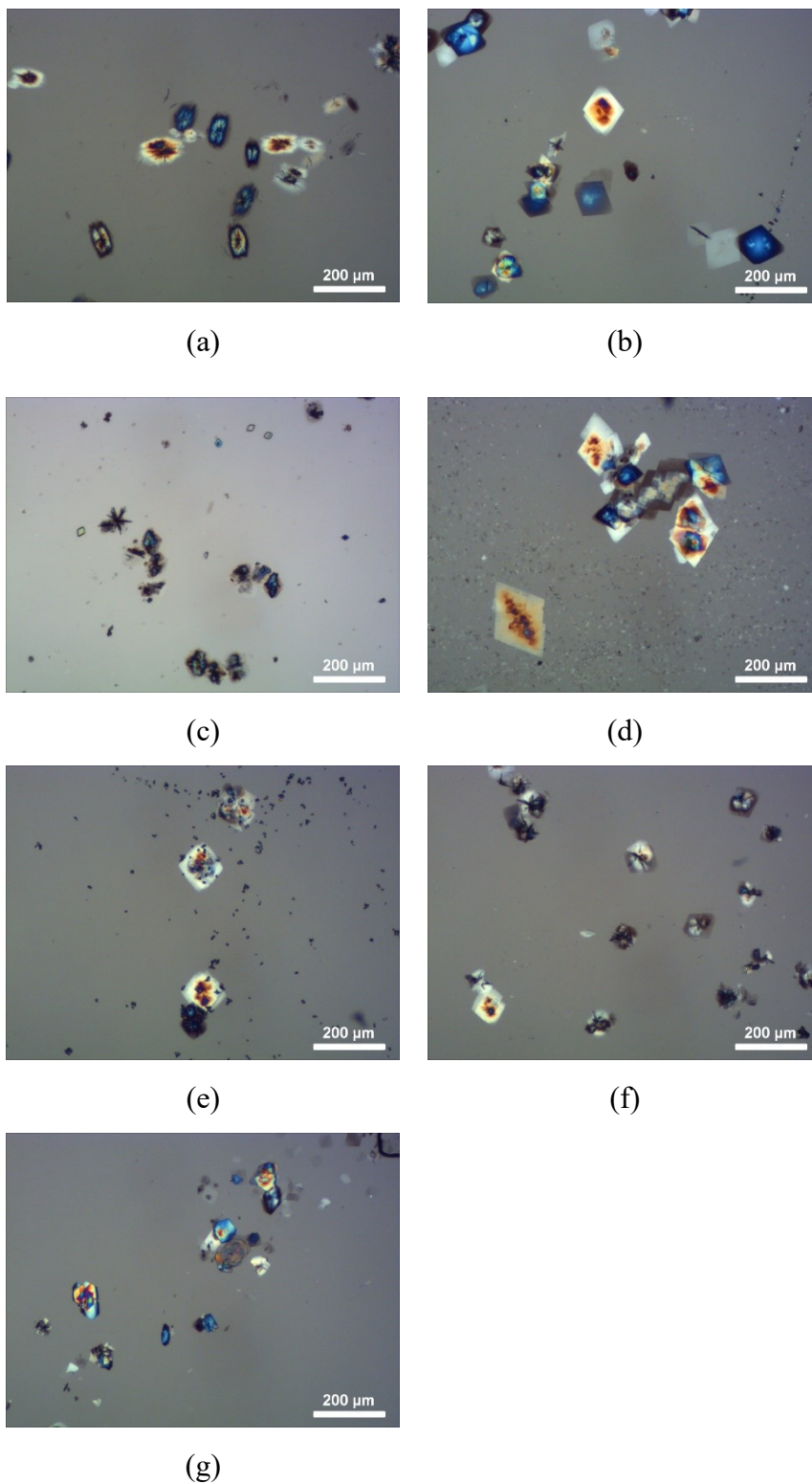


**Figure S4.** OM images of *L*-GLU crystals obtained by antisolvent addition using (a) THF, (b) acetone, (c) 1,4-dioxane, (d) IPA, (e) acetonitrile, (f) ethanol, and (g) methanol.

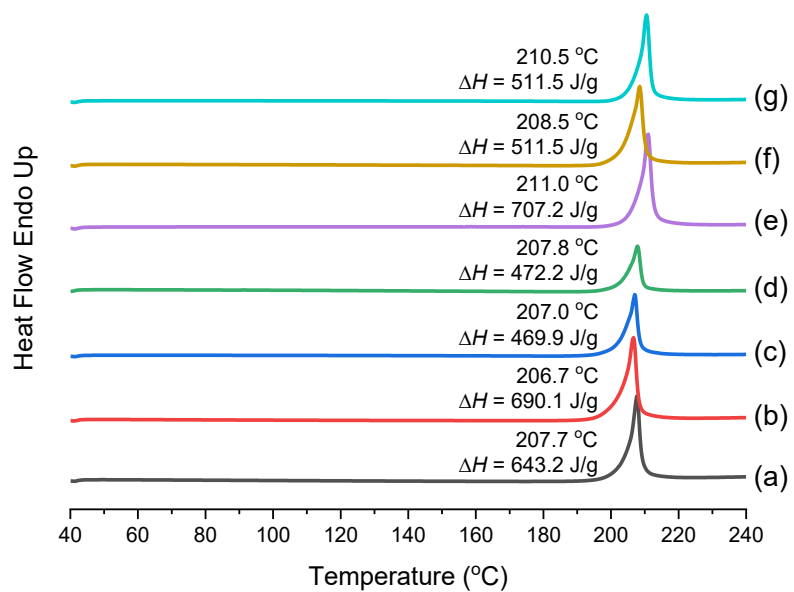


**Figure S5.** DSC scans of *L*-GLU crystals obtained by antisolvent addition using (a) THF, (b) acetone, (c) 1,4-dioxane, (d) IPA, (e) acetonitrile, (f) ethanol, and (g) methanol.

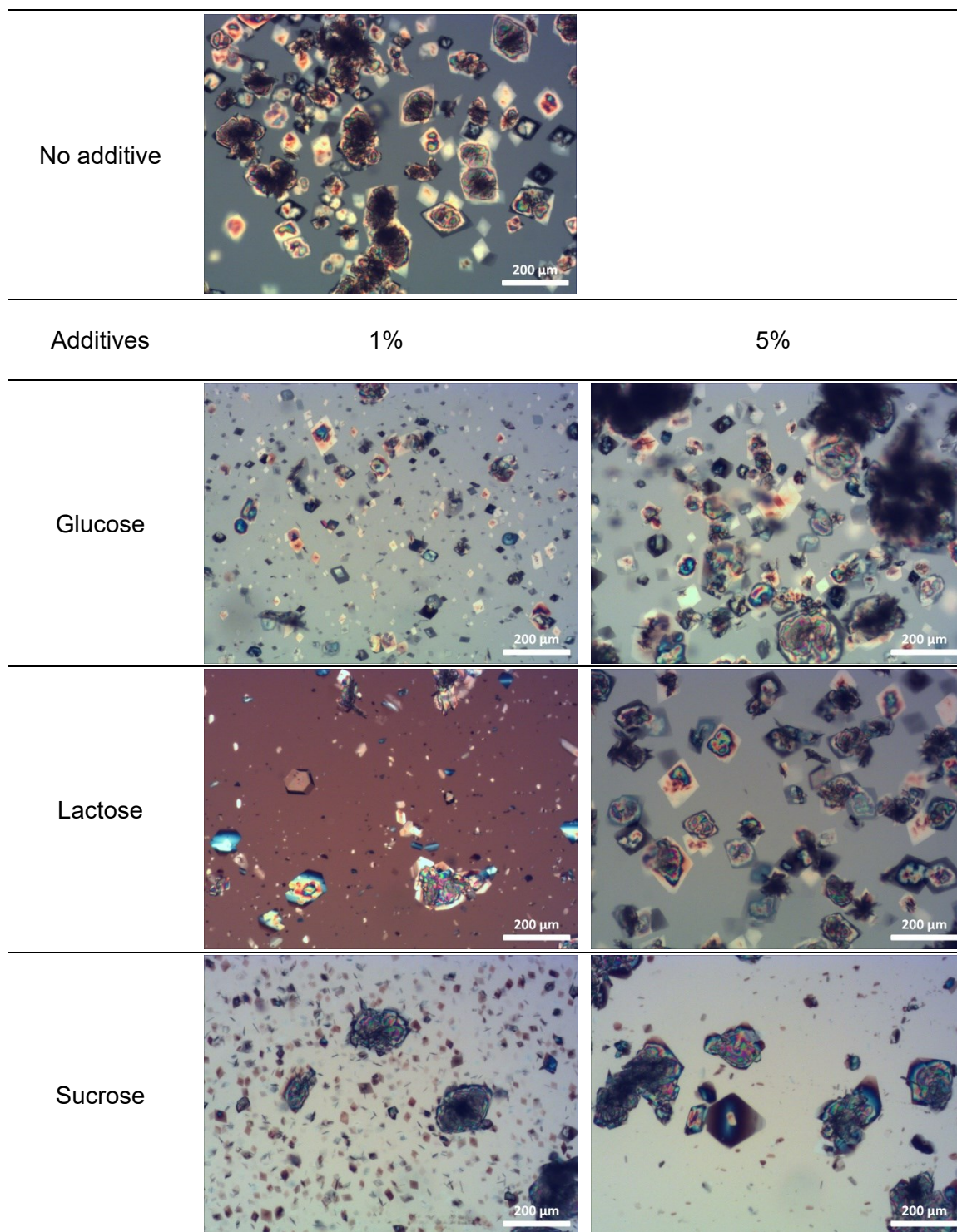


**Figure S6.** OM images of *L*-GLU crystals obtained by reactive crystallization in the absence and presence of glucose, lactose, and sucrose as additives.

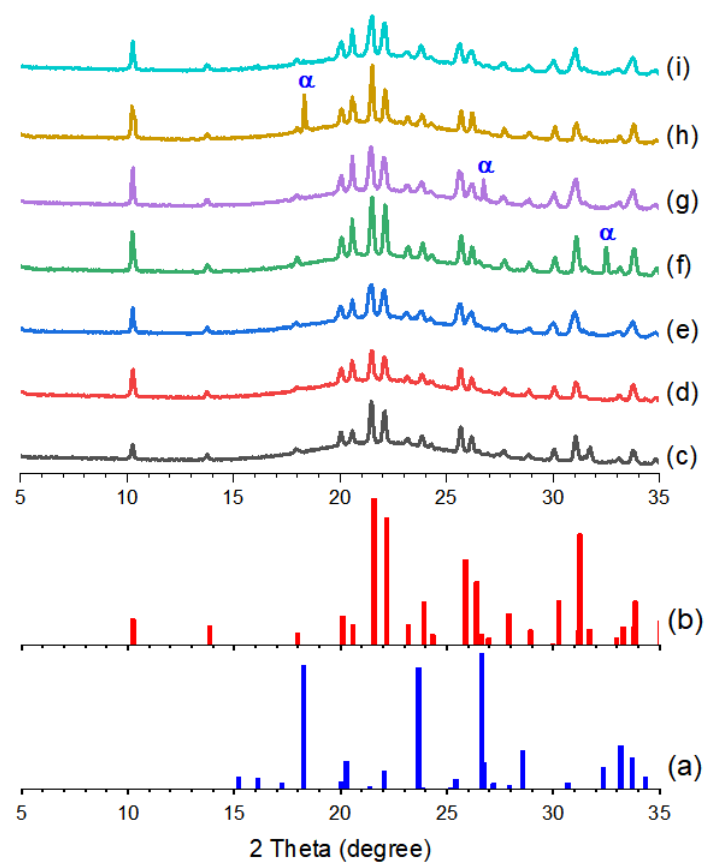


**Figure S7.** Theoretical patterns of (a)  $\alpha$ -GLU and (b)  $\beta$ -GLU acquired from CCDC with CCDC codes: LGLUAC02 and LGLUAC01, respectively. PXR patterns of *L*-GLU crystals obtained by reactive crystallization (c) in the absence and presence of (d) 1% and (e) 5% glucose, (f) 1% and (g) 5% lactose, and (h) 1% and (i) 5% sucrose.

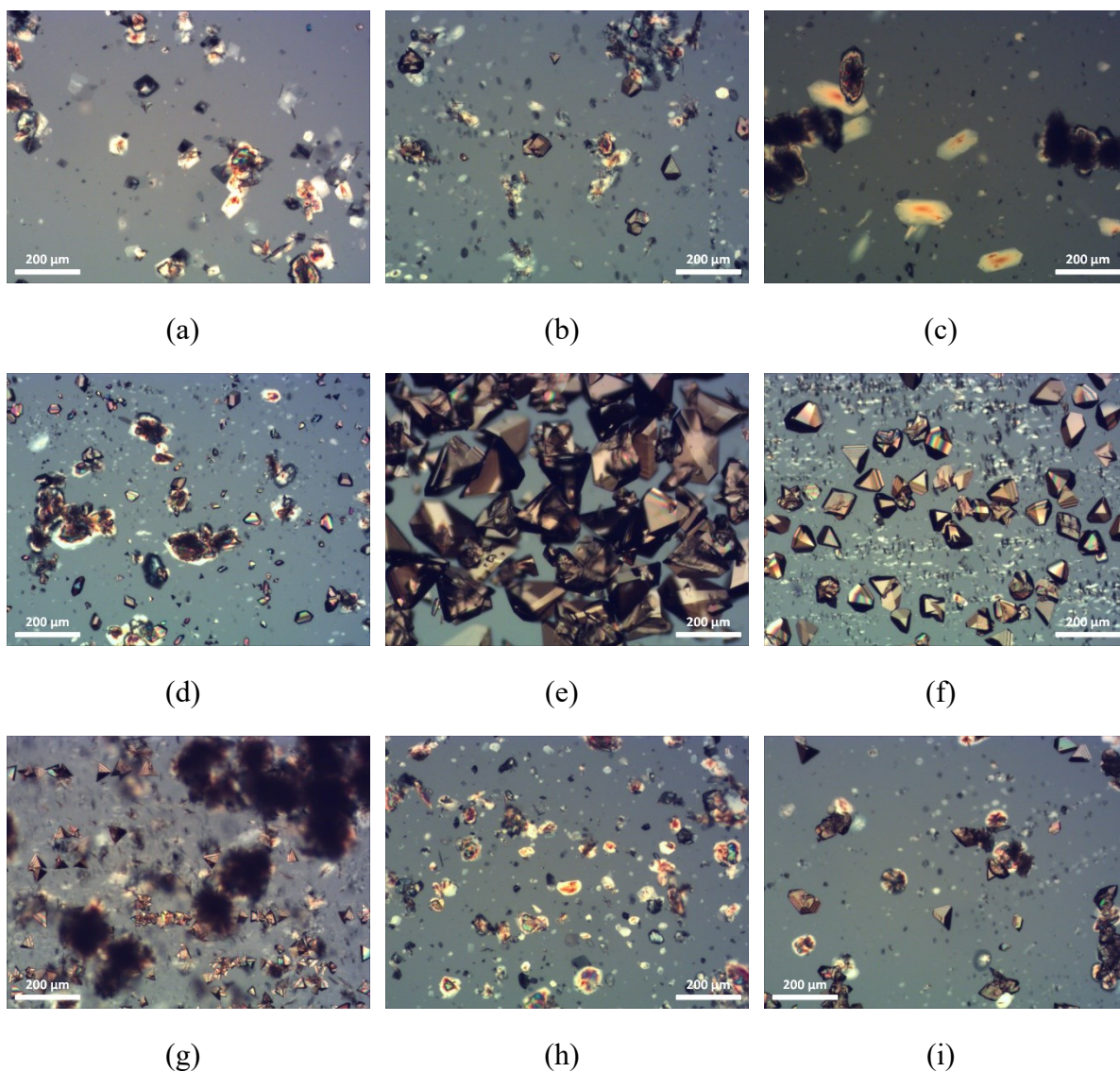


**Figure S8.** OM images of *L*-GLU crystals obtained by reactive crystallization in the presence of (a) glycine, (b) *L*-alanine, (c) *L*-valine, (d) *L*-proline, (e) *L*-leucine, (f) *L*-phenylalanine, (g) *L*-arginine, (h) *L*-serine, and (i) *L*-aspartic acid as additives.

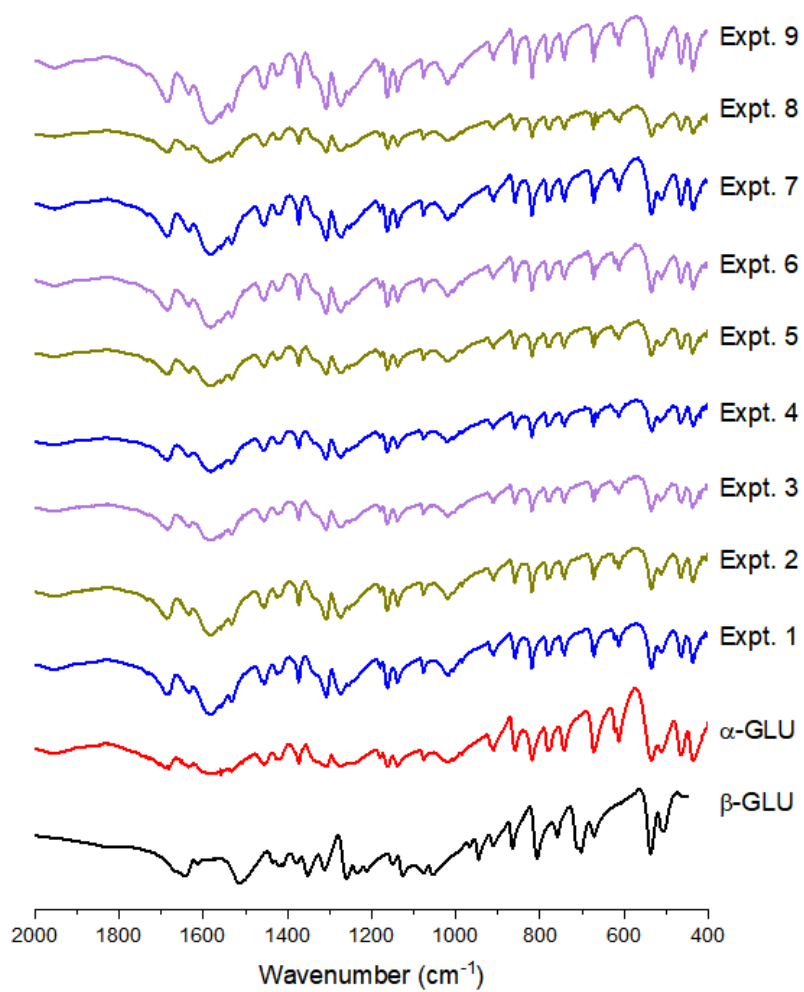


**Figure S9.** FTIR spectra of *L*-GLU crystals obtained by *L*-PHE-assisted reactive crystallization in the Taguchi's method (i.e., Expt. 1 to 9).

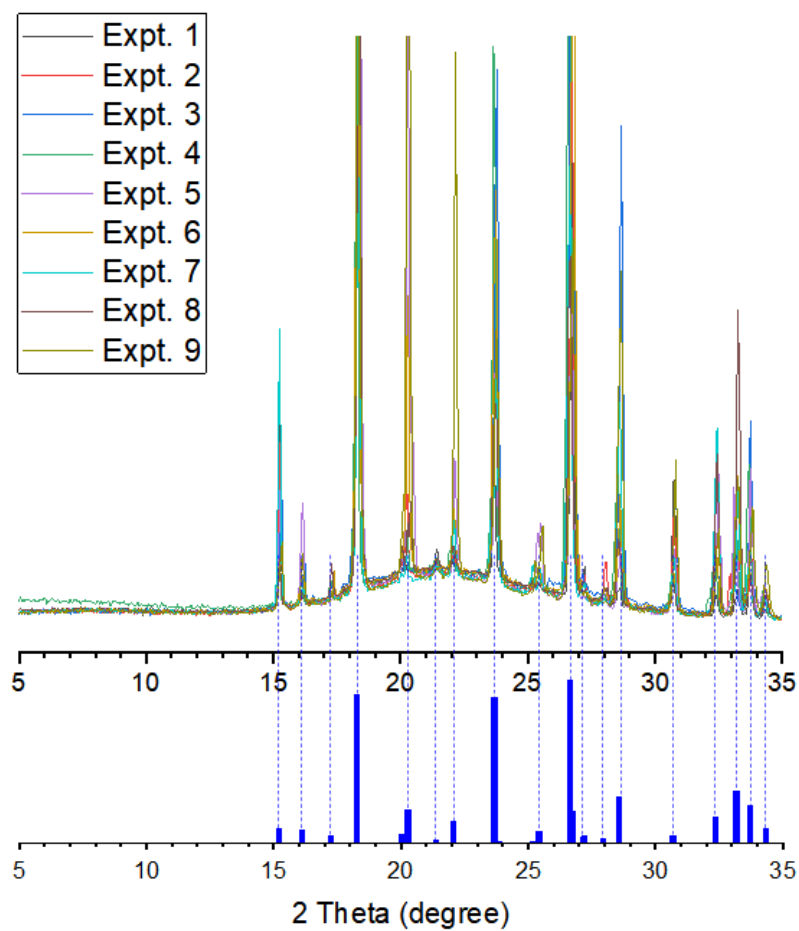


**Figure S10.** Overlapped PXRD spectra of *L*-GLU crystals by *L*-PHE-assisted reactive crystallization in the Taguchi's method (i.e., Expt. 1 to 9). All of them are in good agreement with the theoretical pattern of  $\alpha$ -GLU in the blue column (bottom).

**Table S2.** Response table for S/N ratios with respect to the mean particle size of  $\alpha$ -GLU.

Level	Addition rate of H <sub>2</sub> SO <sub>4</sub> (aq)	Reaction temperature	Agitation rate	Concentration of L-PHE
1	28.55	36.11	23.54	31.94
2	24.69	28.15	32.84	26.78
3	30.01	19.00	26.88	24.54
Delta	5.31	17.09	9.28	7.40
Rank	4	1	2	3

**Table S3.** Response table for S/N ratios with respect to the PSD of  $\alpha$ -GLU.

Level	Addition rate of H <sub>2</sub> SO <sub>4</sub> (aq)	Reaction temperature	Agitation rate	Concentration of L-PHE
1	-42.93	-41.17	-43.97	-43.61
2	-41.13	-41.39	-40.90	-42.23
3	-42.00	-43.49	-41.19	-40.21
Delta	1.80	2.32	3.07	3.40
Rank	4	3	2	1

**Table S4.** Response table for means with respect to the mean particle size of  $\alpha$ -GLU.

<b>Level</b>	<b>Addition rate of H<sub>2</sub>SO<sub>4</sub> (aq)</b>	<b>Reaction temperature</b>	<b>Agitation rate</b>	<b>Concentration of L-PHE</b>
1	167.8	123.9	204.8	193.8
2	158.7	158.0	152.6	170.9
3	182.4	227.0	151.4	144.1
Delta	23.7	103.1	53.3	49.7
Rank	4	1	2	3

**Table S5.** Response table for means with respect to the PSD of  $\alpha$ -GLU.

<b>Level</b>	<b>Addition rate of H<sub>2</sub>SO<sub>4</sub> (aq)</b>	<b>Reaction temperature</b>	<b>Agitation rate</b>	<b>Concentration of L-PHE</b>
1	139.7	113.7	154.3	149.3
2	118.5	120.9	114.7	129.2
3	125.2	148.8	114.5	104.8
Delta	21.2	35.1	39.8	44.5
Rank	4	3	2	1